Author(s): D'Angelo, Stefano

Title: Generalized Moog Ladder Filter: Part I Linear Analysis and Parameterization

Year: 2014

Version: Post print / Accepted author version

**Please cite the original version:**

S. D Angelo and V. Välimäki. Generalized Moog Ladder Filter: Part I Linear Analysis and Parameterization. IEEE Trans. Audio, Speech, and Lang. Process., vol. 22, no. 12, pp. 1825 1832, December 2014.

# Generalized Moog Ladder Filter: Part I – Linear Analysis and Parameterization

Stefano D'Angelo and Vesa Välimäki, *Senior Member, IEEE*

***Abstract*—The Moog ladder filter, which consists of four cascaded first-order ladder stages in a feedback loop, falls within the class of devices that have attracted greatest interest in virtual analog research. On one hand, this work confirms that the presence of exactly four stages in the original analog circuit is motivated by specific filter control issues and, on the other, that such a limitation can be overcome in the digital domain with relative ease. Firstly, a continuous-time large-signal model is defined for a version of the circuit that is generalized to an arbitrary number of ladder stages. Then, the linear behavior of the filter around its natural operating point and the effect of control parameters on the resulting frequency response are studied in depth, to obtain exact analytical expressions for the position of poles in the transfer function and for the dc gain of the filter, as well as a parameterization strategy that is consistent for any number of ladder stages. A previously-introduced linear digital model of the device suggested by Smith is eventually generalized based on these general results, which remain, however, relevant and similarly applicable to other discretizations of the filter. The proposed model faithfully reproduces the linear behavior of the generalized device while providing sensible parametric control for any number of ladder stages.**

***Index Terms*—Acoustic signal processing, circuit simulation, IIR filters, music, resonator filters.**

## I. Introduction

THE Moog ladder filter [1], [2] represents one of the best-known and sought-after analog filters in music technology. Despite its relatively aged design and the wide availability of inexpensive digital alternatives, interest in this device has persisted to date due to its distinctive tonal qualities. Its significance is indeed reflected by the steadily-growing amount of literature dedicated to the topic, especially since the advent of virtual analog modeling [3]–[6]. In addition to the Moog ladder filter, many other filter circuits used in analog music technology have been afterwards converted into the digital form. Examples of such devices include shelving filters [7], [8]; equalizers [7], [9]–[12]; voltage-controlled filters [13], [14]; and tone-control filters used in musical instrument amplifiers [4], [6], [15]–[17].

In technical terms, the Moog ladder filter is a fourth-order resonant low-pass filter implemented through a peculiar ladder circuit topology [1], [2] with embedded nonlinear elements. These nonlinearities produce a distortion that adds a specific and musically-pleasing "warmth" to the output sound. The circuit essentially consists of a differential amplification stage and a series of four low-pass stages, while resonance is generated by feeding back part of the output signal into the input stage. Although the filter circuit has been thoroughly analyzed [18]–[21] and several digital versions have been documented, ranging from linear models [22]–[24] to "heuristic" [25], [26], black-box [27], [28], and physical modeling approaches [18], [21], [29], [30], the simultaneous presence of both multiple nonlinear elements and a global feedback signal path represents a major obstacle in retaining some of the most desirable properties of the original device in the digital domain. The same consideration also applies in the case of other similar devices [31]–[34].

This work is the first in a two-part series that aims to define a new efficient digital structure that draws inspiration from the original Moog ladder filter, generalizing to an arbitrary number of low-pass stages and eventually preserving its linear response, to a large extent, without requiring tuning compensation strategies. In particular, this first paper introduces the circuit, presents a realistic continuous-time large-signal model, and studies its linear behavior in order to obtain analytical expressions relating filter parameters to the resulting frequency response and to determine a parameterization strategy that is consistent for any number of ladder stages.

This paper is organized as follows. Section II presents the generalized filter circuit and its large-signal model based on the derivation in [21]. In Section III, a linearized version of such a model is thoroughly analyzed in the Laplace domain, while Section IV studies the effect of parameterization on the generated frequency response. Section V illustrates the application of the theoretical results to generalize the digital model described in [24], and Section VI eventually concludes the paper.

## II. Generalized Moog Ladder Filter Circuit

The original Moog low-pass ladder circuit [1], [2] essentially consists of a differential amplifier transistor pair in series with four consecutive low-pass stages. The former, as shown in Fig. 1(a), is driven by a subcircuit that can be reasonably approximated by the current source $I_{\mathrm{ctl}}$, whose value depends solely on external control inputs. Each of the latter, as depicted in Fig. 1(b), consists of two transistors whose bases are directly connected and whose emitters are wired through the capacitance $C$.

Manuscript received January 17, 2014. revised May 02, 2014, revised August 07, 2014.

S. D'Angelo is with the Department of Signal Processing and Acoustics, Aalto University, School of Electrical Engineering, P.O. Box 13000, FI-00076 AALTO, Espoo, Finland (email: stefano.d'angelo@aalto.fi).

S. D'Angelo's research is funded by the GETA Graduate School in Electronics, Telecommunications and Automation, and by the Aalto ELEC Doctoral School.

V. Välimäki is with the Department of Signal Processing and Acoustics, Aalto University, School of Electrical Engineering (email: vesa.valimaki@aalto.fi).

The differential pair is fed on one side by the buffered input voltage $V_{\text{in}}$ and on the other by another subcircuit meant to provide a signal that is $k$ times proportional to the phase-inverted and buffered output voltage $\Delta V_4$ across the capacitor of the last low-pass stage, thus introducing a *global feedback* that is responsible for the resonant behavior of the whole filter. The value of $C$ is identical for all low-pass stages, and each transistor base couple is also connected to a corresponding output terminal of a multiple-load voltage divider subcircuit that powers the filter. Furthermore, the transistor collectors of the last stage are also connected to each other and to the positive terminal of the voltage source in the power subcircuit.

A common improvement to this and other similar circuits is represented by the possibility to choose different frequency response modes based on which stages the output voltage is extracted from and fed back to the differential pair [26]. It is, then, possible to generalize the circuit to any positive number $N$ of ladder stages, as shown in in Fig. 2. A continuous-time large-signal model of such a generalized circuit can be easily obtained by following the same reasoning as in [21], under the assumption that the current gain factor (*beta*) of the transistors can be considered infinite, which in turn implies that all base currents are null and that the base voltages of ladder stages are constant. The resulting model can be expressed as

$$\frac{\mathrm{d}\Delta V_i}{\mathrm{d}t} = \frac{I_{\text{ctl}}}{2C}\left[\tanh\left(\frac{\Delta V_{i-1}}{2V_{\text{T}}}\right) - \tanh\left(\frac{\Delta V_i}{2V_{\text{T}}}\right)\right], \quad (1)$$

for $i > 1$, while

$$\frac{\mathrm{d}\Delta V_1}{\mathrm{d}t} = -\frac{I_{\text{ctl}}}{2C}\left[\tanh\left(\frac{\Delta V_1}{2V_{\text{T}}}\right) + \tanh\left(\frac{V_{\text{in}} + k\Delta V_N}{2V_{\text{T}}}\right)\right], \quad (2)$$

where $V_{\text{T}}$ is the thermal voltage ($\approx 26\,\text{mV}$ at room temperature $300\,\text{K}$).

## III. Linear Analysis

While the linear response of the Moog ladder filter has been already studied in previous works, e.g. [19], [22], the exact relationships between user-controlled parameters and the position of filter poles have been so far only partially analyzed in [20], but otherwise mostly neglected. This, however, represents a crucial aspect in understanding the behavior of the original filter and is here regarded as a prerequisite to effectively define analogous digital structures. A similar approach in the case of another circuit was taken in [13]. The analysis contained in this section applies to the generalized circuit introduced in Section II.

When a null input signal $V_{\text{in}} = 0$ is fed into the system, the derivatives in (1) and (2) are null, hence $\Delta V_N = \Delta V_{N-1} = \ldots = \Delta V_1 = -k\Delta V_N \Rightarrow \Delta V_i = 0$ is the operating point of each stage $i$. It is therefore possible to linearize $\tanh(x) \approx x$ around $x_0 = 0$, leading to

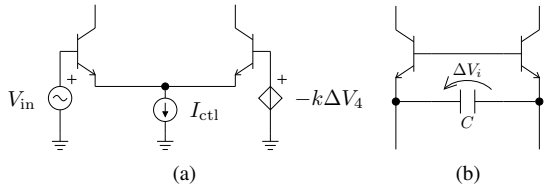


Fig. 1. (a) Differential pair and (b) ladder stage.

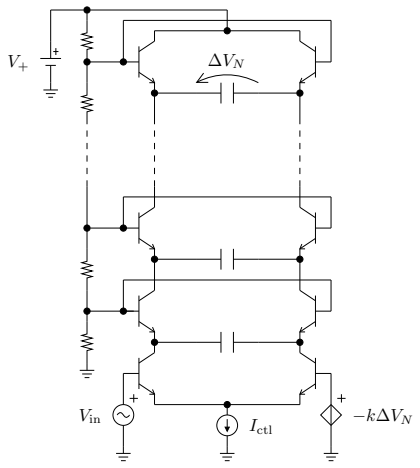


Fig. 2. Generalized ladder filter circuit.

$$\frac{\mathrm{d}\Delta V_1}{\mathrm{d}t} = -\frac{I_{\text{ctl}}}{4CV_{\text{T}}}\left(\Delta V_1 + V_{\text{in}} + k\Delta V_N\right), \quad (3)$$

$$\frac{\mathrm{d}\Delta V_i}{\mathrm{d}t} = \frac{I_{\text{ctl}}}{4CV_{\text{T}}}\left(\Delta V_{i-1} - \Delta V_i\right), \quad (4)$$

which can be transformed to the Laplace domain as

$$\frac{\Delta V_1(s)}{V_{\text{in}}(s) + k\Delta V_N(s)} = -\frac{\frac{I_{\text{ctl}}}{4CV_{\text{T}}}}{s + \frac{I_{\text{ctl}}}{4CV_{\text{T}}}}, \quad (5)$$

$$\frac{\Delta V_i(s)}{\Delta V_{i-1}(s)} = \frac{\frac{I_{\text{ctl}}}{4CV_{\text{T}}}}{s + \frac{I_{\text{ctl}}}{4CV_{\text{T}}}}, \qquad \text{for } i > 1, \quad (6)$$

from which the global transfer function can be derived as

$$\frac{\Delta V_N(s)}{V_{\text{in}}(s)} = -\frac{\left(\frac{I_{\text{ctl}}}{4CV_{\text{T}}}\right)^N}{\left(s + \frac{I_{\text{ctl}}}{4CV_{\text{T}}}\right)^N + k\left(\frac{I_{\text{ctl}}}{4CV_{\text{T}}}\right)^N}, \quad (7)$$

and the denominator can be factorized to find the explicit positions of the poles:

$$\frac{\Delta V_N(s)}{V_{\text{in}}(s)} = -\frac{\left(\frac{I_{\text{ctl}}}{4CV_{\text{T}}}\right)^N}{\prod_{u=0}^{N-1}\left[s + \frac{I_{\text{ctl}}}{4CV_{\text{T}}}\left(1 - \sqrt[N]{k}e^{j\frac{(2u+1)\pi}{N}}\right)\right]}. \quad (8)$$

It is then possible to combine together the expressions of complex conjugate poles, thus obtaining

$$\frac{\Delta V_N(s)}{V_{\text{in}}(s)} = -\frac{\left(\frac{I_{\text{ctl}}}{4CV_{\text{T}}}\right)^N}{\left(s + 2\pi f_{\text{c,odd}}\right)^{N-2\lfloor N/2\rfloor}\prod_{w=0}^{\lfloor N/2\rfloor - 1} H_w(s)}, \quad (9)$$

with

$$H_w(s) = s^2 + \frac{2\pi f_{c,w}}{Q_w} s + (2\pi f_{c,w})^2, \tag{10}$$

$$f_{c,\mathrm{odd}} = \frac{1 + \sqrt[N]{k}}{8\pi C V_T} I_{ctl}, \tag{11}$$

$$f_{c,w} = \frac{A_w(k)}{8\pi C V_T} I_{ctl}, \tag{12}$$

$$Q_w = \frac{A_w(k)}{2B_w(k)}, \tag{13}$$

$$A_w(k) = \sqrt{1 + \sqrt[N/2]{k} - 2\sqrt[N]{k}\cos\left(\frac{(2w+1)\pi}{N}\right)}, \tag{14}$$

$$B_w(k) = 1 - \sqrt[N]{k}\cos\left(\frac{(2w+1)\pi}{N}\right), \tag{15}$$

where $w = 0, 1, ..., \lfloor N/2 \rfloor - 1$ is the pole-pair index.

Therefore, when $k = 0$ the filter will exhibit one pole of order $N$ at $s = -\frac{I_{ctl}}{4CV_T}$ for any $N$, otherwise, excluding the trivial case $N = 1$, there will be $\lfloor N/2 \rfloor$ distinct pairs of first-order complex conjugate poles lying on the circumference with radius $\sqrt[N]{k}\frac{I_{ctl}}{4CV_T}$ and center $\left(-\frac{I_{ctl}}{4CV_T}, 0\right)$, plus one more real pole, if $N$ is odd, at $s = -\frac{1+\sqrt[N]{k}}{4CV_T} I_{ctl}$. Fig. 3 shows the positions of poles for different values of $k$ in the cases $N = 4$ and $N = 5$. Furthermore, the dc gain can be easily derived from (7) by substituting $s = 0$, obtaining

$$g_{dc} = -\frac{1}{1+k}. \tag{16}$$

It is interesting to notice how the value of $I_{ctl}$ only affects the cut-off frequency $f_{c,w}$ of each couple of complex conjugate poles, as well as $f_{c,\mathrm{odd}}$ if $N$ is odd, while the feedback coefficient $k$ influences $f_{c,w}$, $f_{c,\mathrm{odd}}$, $Q_w$, and the dc gain $g_{dc}$. Also, $g_{dc}$ does not depend on $N$.

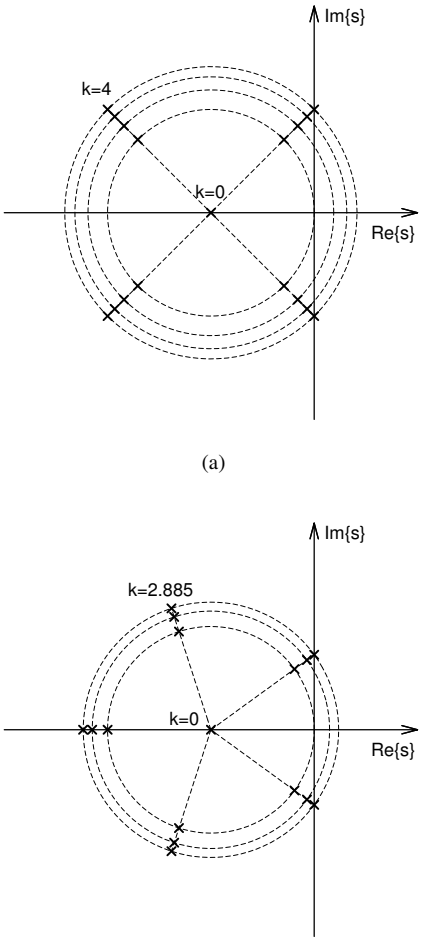


Fig. 3. Positions of poles with (a) $N = 4$, $k = 0, 1, 2, 3, 4$, and (b) $N = 5$, $k = 0, 1, 2, \sec^5(\pi/5)$.

## IV. Parameterization

The original device is mainly controlled by two parameters, namely a cut-off frequency parameter, which does not always correspond to the frequency of any of the filter poles, as detailed later on, and feedback loop gain, which instead corresponds to $k$. This section explores various parameterization strategies and their relationships with the resulting frequency responses for any choice of $N$.

### A. Filter Parameters and Frequency Response

When $N = 1$, the global feedback loop does not introduce resonance and the cut-off frequency of the filter is

$$f_c \triangleq f_{c,\mathrm{odd}} = \frac{1+k}{8\pi C V_T} I_{ctl}, \tag{17}$$

otherwise, for $N \geq 2$, the cut-off frequency $f_c$ and quality factor $Q$ of the leading poles are defined by

$$f_c \triangleq f_{c,0} = \frac{A_0(k)}{8\pi C V_T} I_{ctl}, \tag{18}$$

$$Q \triangleq Q_0 = \frac{A_0(k)}{2B_0(k)}, \tag{19}$$

where $A_0(k)$ and $B_0(k)$ are obtained from (14) and (15), respectively, by setting $w = 0$. More conveniently, the cut-off frequency can be expressed for any $N$ as

$$f_c = \frac{\alpha(k)}{8\pi C V_T} I_{ctl}, \tag{20}$$

with

$$\alpha(k) = \begin{cases} 1 + k, & \text{when } N = 1, \\ A_0(k), & \text{when } N \geq 2. \end{cases} \tag{21}$$

Conversely, $I_{ctl}$ can be expressed in terms of $f_c$ and $\alpha(k)$ for any $N$, as well as $k$ in terms of $Q$ for $N \geq 2$ as

$$I_{ctl} = \frac{8\pi C V_T}{\alpha(k)} f_c, \tag{22}$$

$$k = \left[\frac{\left(4Q^2 - 1\right)\cos\left(\frac{\pi}{N}\right) - \sqrt{4Q^2 - 1}\sin\left(\frac{\pi}{N}\right)}{4Q^2\cos^2\left(\frac{\pi}{N}\right) - 1}\right]^N. \tag{23}$$

Equations (18), (19), (22), and (23) describe both-way mappings between directly-controllable filter parameters, namely $I_{ctl}$ and $k$, and characterizing properties of the leading poles of the filter, namely $f_c$ and, in the case $N \geq 2$.

Furthermore, for $N \geq 2$, from (23),

$$k_{\max} = \lim_{Q \to +\infty} k = \sec^N\left(\frac{\pi}{N}\right) \tag{24}$$

defines the upper-bound limit of $k$ for the filter to be stable, i.e., $k \in [0, k_{\max}]$, while, from (19),

$$Q_{\min} = Q|_{k=0} = \frac{1}{2}, \tag{25}$$

thus $Q \in \left[\frac{1}{2}, +\infty\right)$. Note that $k_{\max}$ is finite for $N \geq 3$, while given the absence of resonant behavior when $N = 1$, it can be regarded as being infinite. In the real device, $k_{\max}$ actually represents the lower-bound value by which the filter starts to self-oscillate due to its embedded nonlinearities.

### B. Filter Order and Parameterization

The choice $N = 4$ in the original analog device is motivated in [2] by considering that a phase-shift oscillator produces a sinusoidal signal whose frequency corresponds to a phase shift of 180 degrees, which can only match the cut-off frequency of a series of identical RC low-pass filters in its feedback branch if $N = 4$, since each provides 45 degrees of phase shift at said frequency. Furthermore, with such a choice of $N$, resonance typically occurs at a frequency that does not vary dramatically with $k$. A property shared by all choices of $N$ is that the cut-off slope does not change in position w.r.t. $k$. It is interesting to notice that the particular choice of $N$ in the analog filter, at least as far as documented in the literature, is mainly related to its parametric control and not to the filter roll-off. This subsection studies these issues in order to understand the implications when choosing a given parameterization strategy for any choice of $N$.

Firstly, we define the *natural cut-off frequency* of the filter, the cut-off frequency when $k = 0$, as

$$\widehat{f_c} \triangleq f_c|_{k=0} = \frac{I_{\text{ctl}}}{8\pi C V_{\text{T}}} = \frac{f_c}{\alpha(k)}, \tag{26}$$

which is linearly proportional to the directly-controllable parameter $I_{\text{ctl}}$. We also introduce a relative cut-off frequency error measure

$$\epsilon_{\text{r,c}}(k) \triangleq \left|\frac{f_c - \widehat{f_c}}{f_c}\right| = \left|1 - \frac{1}{\alpha(k)}\right|, \tag{27}$$

which can be shown to be monotonically increasing for $N \leq 2$, while it tends to 1 as $k \to \infty$ for any $N$. Furthermore, when $N \geq 3$, it has a local maximum at $k = \cos^N\left(\frac{\pi}{N}\right)$ of value $\csc\left(\frac{\pi}{N}\right) - 1$, which is strictly greater than 1 for $N \geq 7$.

Summing up, the absolute maximum of the relative cut-off frequency error is

$$\epsilon_{\text{r,c,max}} = \begin{cases} 1, & \text{when } N \leq 6, \\ \csc\left(\frac{\pi}{N}\right) - 1, & \text{when } N \geq 7. \end{cases} \tag{28}$$

Fig. 4 visualizes this measure for $N = 3, ..., 8$ w.r.t. the normalized feedback gain

$$k_{\text{norm}} \triangleq \frac{k}{k_{\max}} = k\cos^N\left(\frac{\pi}{N}\right), \tag{29}$$

clearly showing that such error is always significant for any choice of $N$, even when $k \in [0, k_{\max}]$. Note that, when $N = 4$ and $k_{\text{norm}} = 1$, the error $\epsilon_{\text{r,c}} = 0$, which is consistent with the reasoning on phase-shift oscillators at the beginning of this subsection.

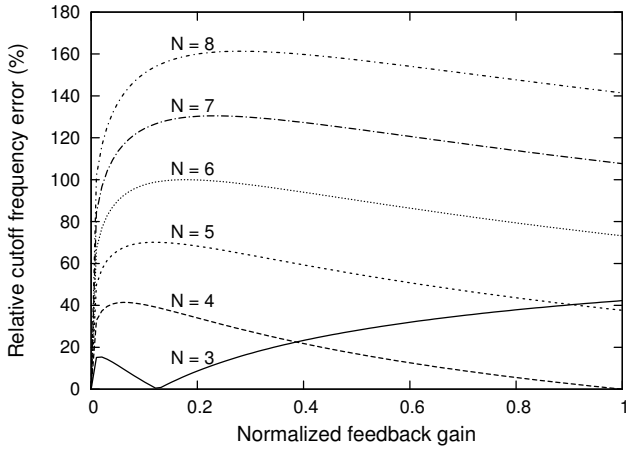


Fig. 4. Relative cut-off frequency error $\epsilon_{\text{r,c}}$, in percentage, w.r.t. normalized feedback gain $k_{\text{norm}}$ for $N = 3, ..., 8$.

It is, then, possible to show that the oblique asymptote in the Bode plot of the magnitude response of the filter for $\omega \to \infty$ can be expressed as

$$20\log_{10}\left|\frac{\Delta V_N(j\omega)}{V_{\text{in}}(j\omega)}\right| \to -20N\log_{10}(\omega) + 20N\log_{10}(2\pi\widehat{f_c}) \tag{30}$$

for any $N$. This expression, which characterizes the cut-off slope position, does not depend on $k$. If, instead, the filter is parameterized in terms of the actual cut-off frequency $f_c$, this property is lost, and since, according to (26), $\widehat{f_c} = f_c/A_0(k)$, we can define the relative gain of the resulting cut-off slope over the "normal" result as

$$\Delta g_\infty = \frac{1}{\alpha^N(k)}, \tag{31}$$

corresponding to a relative cut-off slope gain error

$$\epsilon_{\text{r,s}}(k) \triangleq |1 - \Delta g_\infty| = \left|1 - \frac{1}{\alpha^N(k)}\right|, \tag{32}$$

which is obviously greater than $\epsilon_{\text{r,c}}(k)$ for $N \geq 2$, and increasingly so at higher filter orders.

Finally, unlike other common resonant low-pass filter topologies, such as Sallen-Key and state variable filters [35], the dc gain depends on the value of $k$, as described by (16). Such a property of the analog device could be either considered as a desirable feature, since it corresponds to a rough form of filter normalization [35], or as a shortcoming, in which case it is possible to define a relative dc gain error measure

$$\epsilon_{\text{r,dc}}(k) \triangleq |1 + g_{\text{dc}}| = \left|1 - \frac{1}{1+k}\right|. \tag{33}$$

### C. Choosing a Parameterization Strategy

As discussed in the previous subsection, the choice $N = 4$ in the original device is based on considerations related to parametric filter control. Unluckily, the filter behavior varies

significantly between different filter orders, and hence it is reasonable to consider cautious modifications to achieve some degree of consistency in parametric control across all values of $N$.

While the original filter is effectively controlled in terms of $I_{\mathrm{ctl}}$, which is proportional to $\widehat{f}_{\mathrm{c}}$, and $k$, a possibility worth examining consists in parameterizing in terms of $f_{\mathrm{c}}$ rather than $I_{\mathrm{ctl}}$. In this case, the resonant frequency exactly matches the user-controllable setting, thus achieving complete decoupling from the $k$ parameter. Such orthogonality of controls is most likely to be regarded as an improvement to the behavior of the original device, even though that is not always true in virtual analog modeling [15]. Furthermore, since such a change is limited to the control part of the filter, no modification to the audio path is needed, neither in the analog nor digital domain. Also note that the dc gain remains unaffected. The only concrete drawback resides in the introduction of a generally significant cut-off slope gain error, as outlined in the previous subsection, which can, however, be otherwise interpreted as an $N$- and $k$-dependent passband modification. Figs. 5(a) and 6(a) show the magnitude responses of the fourth-order ($N = 4$) and eight-order ($N = 8$) filters, respectively, with a fixed value of $\widehat{f}_{\mathrm{c}}$ and different values of $k$, while Figs. 5(b) and 6(b) visualize the same results for a fixed $f_{\mathrm{c}}$ value.

It would also be possible to apply an $N$- and $k$-dependent gain factor to the audio signal to either compensate for the cut-off slope gain error or to render the dc gain constant. In the first case, the effect on the resulting magnitude responses would be dramatic enough, in the general case, to make such an adjustment impractical, as shown in Figs. 5(c) and, especially, 6(c). In the latter case, the compensation would worsen the the resulting cut-off slope gain error, as is evident from Figs. 5(d) and 6(d), and it would also be arguable whether the compensation would represent a real improvement. Moreover, it would also be unclear where it should be applied in the audio signal path, and especially when considering the nonlinear behavior of the filter.

On the other hand, the choice of parameterizing the feedback loop gain in terms of $k$, $k_{\mathrm{norm}}$, when possible, or $Q$, does not affect the resulting magnitude responses. However, the infinite range of $Q$ and its nontrivial mapping to $k$ (19) most likely represent undesirable complications. Furthermore, nonlinear emulators may let the user exceed $k_{\max}$ in order to establish self-oscillation, which is not possible to achieve through $Q$-based control. Based on the considerations discussed so far, we suggest parameterizing in terms of $f_{\mathrm{c}}$ and $k$ without any gain compensation.

## V. Digital Implementation Example

This section presents a digital filter design that provides a linear implementation of the generalized device, based on a series of biquad filters and, in case $N$ is odd, a final first-order section. As such, the design essentially represents a generalization and reparameterization of the biquad-based design described in [24]. While several other linear filter structures have also been proposed for discretizing the original device [3], [22], [23], the present one was mainly chosen for its conceptual simplicity. In any case, the results obtained from previous analyses can be similarly applied to generalize and reparameterize any linear digital model of the original device.

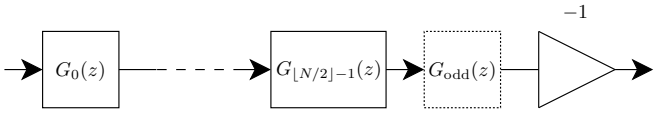


Fig. 7. Proposed filter design. The dotted $G_{\mathrm{off}}(z)$ block is only present when $N$ is odd.

Fig. 7 shows a block-diagram representation of the proposed design. The input signal is fed into a series of $\lfloor N/2 \rfloor$ generally different biquad filters, each implementing the transfer function

$$G_w(s) \triangleq \frac{\frac{I_{\mathrm{ctl}}}{4CV_{\mathrm{T}}}}{H_w(s)} = \frac{\frac{2\pi f_{\mathrm{c}}}{A_0(k)}}{s^2 + 4\pi f_{\mathrm{c}} \frac{B_w(k)}{A_0(k)} s + \left(2\pi f_{\mathrm{c}} \frac{A_w(k)}{A_0(k)}\right)^2}, \tag{34}$$

for $w = 0, 1, ..., \lfloor N/2 \rfloor - 1$, which corresponds in the $z$ domain, by applying the bilinear transform with pre-warping around $f_{\mathrm{c}}$, to

$$G_w(z) = \frac{b_{0,w}\left(1 + z^{-1}\right)^2}{1 + a_{1,w} z^{-1} + a_{2,w} z^{-2}}, \tag{35}$$

where

$$a_{1,w} = 2\frac{{A_w}^2(k) D^2 - {A_0}^2(k)}{E_w(k)}, \tag{36}$$

$$a_{2,w} = 1 - \frac{4A_0(k) B_w(k) D}{E_w(k)}, \tag{37}$$

$$b_{0,w} = \frac{D^2}{E_w}, \tag{38}$$

$$D = \tan\left(\pi \frac{f_{\mathrm{c}}}{f_{\mathrm{s}}}\right), \tag{39}$$

$$E_w(k) = {A_w}^2(k) D^2 + 2A_0(k) B_w(k) D + {A_0}^2(k), \tag{40}$$

and $f_{\mathrm{s}}$ is the sample rate.

When $N$ is odd, the signal also goes through a filter implementing

$$G_{\mathrm{odd}}(s) \triangleq \frac{\frac{I_{\mathrm{ctl}}}{4CV_{\mathrm{T}}}}{s + 2\pi f_{\mathrm{c,odd}}} = \frac{\frac{2\pi f_{\mathrm{c}}}{\alpha(k)}}{s + \frac{2\pi f_{\mathrm{c}}}{\alpha(k)}\left(1 + \sqrt[N]{k}\right)}, \tag{41}$$

which, applying the same Laplace-to-$z$-domain mapping, corresponds to

$$G_{\mathrm{odd}}(z) = \frac{b_{0,\mathrm{odd}}\left(1 + z^{-1}\right)}{1 + a_{1,\mathrm{odd}} z^{-1}}, \tag{42}$$

where

$$a_{1,\mathrm{odd}} = \frac{\left(1 + \sqrt[N]{k}\right) D - \alpha(k)}{\left(1 + \sqrt[N]{k}\right) D + \alpha(k)}, \tag{43}$$

$$b_{0,\mathrm{odd}} = \frac{D}{\left(1 + \sqrt[N]{k}\right) D + \alpha(k)}. \tag{44}$$

A sign-inverting element completes the proposed design in order to match the output phase of the analog device.

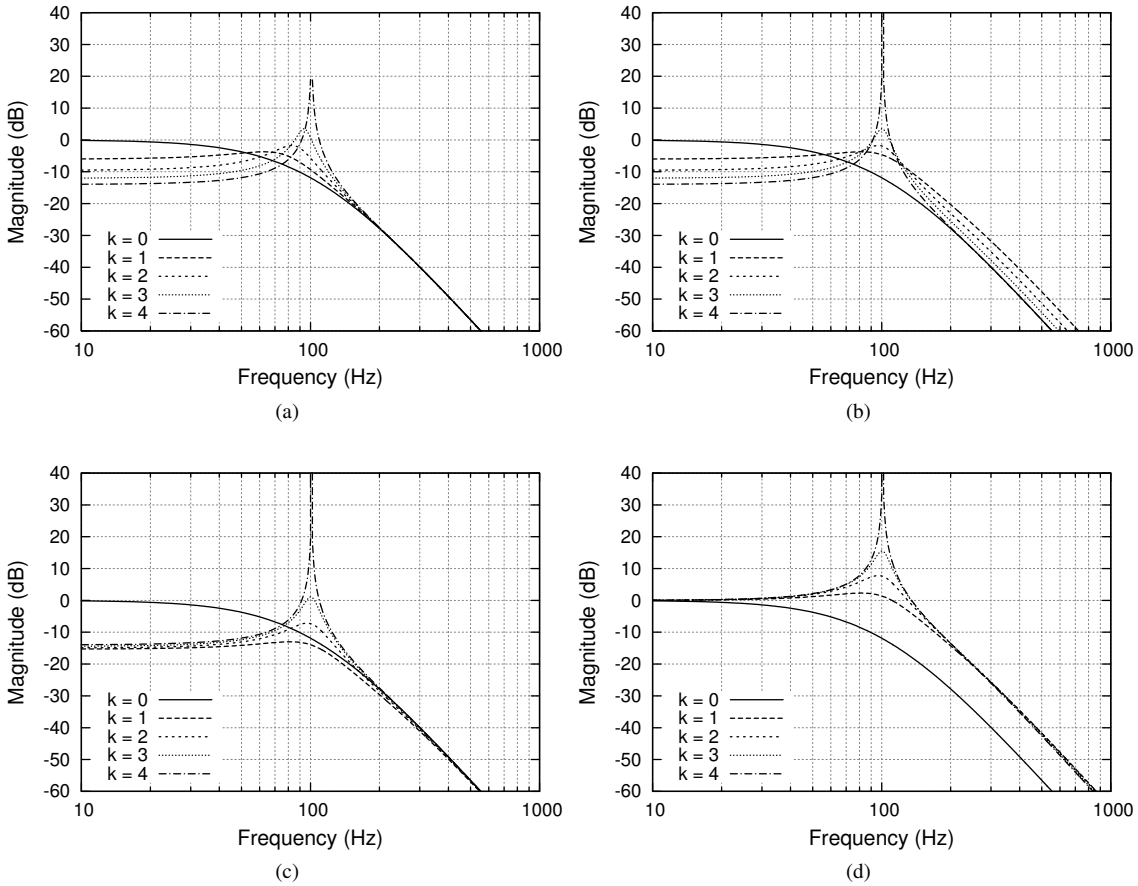


Fig. 5. Magnitude responses of the fourth-order ($N = 4$) filter with $k = 0, 1, 2, 3, 4$ and (a) $\widehat{f_c} = 100\,\text{Hz}$, (b) $f_c = 100\,\text{Hz}$, (c) $f_c = 100\,\text{Hz}$ and cut-off-slope-gain compensation, and (d) $f_c = 100\,\text{Hz}$ and relative dc gain compensation.

The various filter blocks can be actually implemented by any compatible realization. For example, w.r.t. the biquad sections, employing direct form structures [36] leads to minimally-demanding algorithms in terms of number of audio-rate operations or memory usage, while such advantages can be traded with enhanced time-varying stability and reduced output noise by adopting, e.g., normalized ladder or coupled form structures [37]. In any case, whatever the chosen filter realization, and within the limits imposed by finite wordlength effects, the generated frequency responses will match those obtained from the analog device, with the only inconvenience represented by frequency-warping at high frequencies due to the bilinear transform, which increases the $Q$ of the resonance, as shown in Fig. 8 in the case $N = 4$. The cut-off frequency and gain will not be affected by frequency-warping, but are exact at all frequencies.

## VI. Conclusions

This paper analyzed a generalized version of the Moog ladder filter circuit. Its continuous-time large-signal model was derived, and linear analysis was performed around its operating point, with emphasis on the effects of the global feedback, yielding exact analytical expressions for the position of poles in the transfer function and for the dc gain of the filter. The study of the effects of the original filter parameters on the resulting frequency responses theoretically confirmed, on one hand, the validity of the motivations given in [2] for the choice of exactly four ladder stages in the analog design, and on the other allowed to establish analytical error measures relating certain parameterization and gain compensation strategies to desirable linear filter behavior. On the basis of these considerations, it was suggested to employ a parameterization based on the frequency cut-off of the leading poles of the filters in the digital domain, so as to provide sensible parametric control for any number of ladder stages. As an example, such a filter control strategy was applied to generalize the filter model described in [24], obtaining a family of digital structures that faithfully reproduces the linear behavior of the analog device and only suffers from frequency-warping at high frequencies due to the bilinear transform.

## Acknowledgment

We acknowledge fruitful discussions with Dr. Julian Parker.

## References

[1] R. A. Moog, "A voltage-controlled low-pass high-pass filter for audio signal processing," in *Proc. 17th AES Convention*, New York, USA, October 1965.

[2] ——, "Electronic high-pass and low-pass filters employing the base to emitter diode resistance of bipolar transistors," October 1969, U.S. Patent 3,475,623.

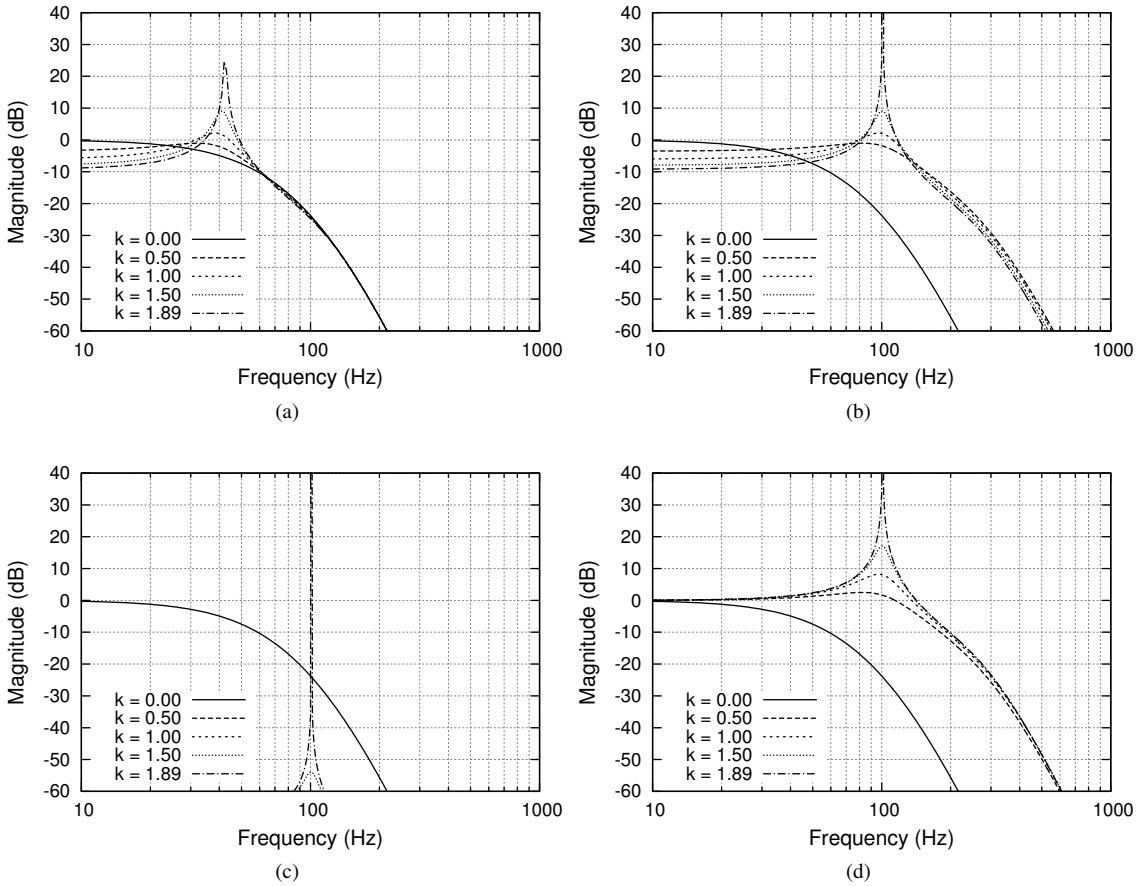


Fig. 6. Magnitude responses of the eight-order ($N = 8$) filter with $k = 0, 1/2, 1, 3/2, \sec^8(\pi/8)$ and (a) $\widehat{f_c} = 100\,\text{Hz}$, (b) $f_c = 100\,\text{Hz}$, (c) $f_c = 100\,\text{Hz}$ and cut-off-slope-gain compensation, and (d) $f_c = 100\,\text{Hz}$ and relative dc gain compensation.


[3] T. Stilson, "Efficiently-variable non-oversampled algorithms in virtual-analog music synthesis," Ph.D. dissertation, Stanford University, Stanford, CA, USA, June 2006, available online at https://ccrma.stanford.edu/~stilti/papers/TimStilsonPhDThesis2006.pdf.

[4] D. T. Yeh, "Digital implementation of musical distortion circuits by analysis and simulation," Ph.D. dissertation, Stanford University, Stanford, CA, USA, June 2009, available online at https://ccrma.stanford.edu/~dtyeh/papers/DavidYehThesissinglesided.pdf.

[5] V. Välimäki, F. Fontana, J. O. Smith, and U. Zölzer, "Introduction to the special issue on virtual analog audio effects and musical instruments," *IEEE Trans. Audio, Speech and Lang. Process.*, vol. 18, no. 4, pp. 713–714, May 2010.

[6] V. Välimäki, S. Bilbao, J. O. Smith, J. S. Abel, J. Pakarinen, and D. Berners, "Virtual analog effects," in *DAFX: Digital Audio Effects, Second Edition*, U. Zölzer, Ed. Chichester, UK: Wiley, 2011, pp. 473–522.

[7] P. A. Regalia and S. K. Mitra, "Tunable digital frequency response equalization filters," *IEEE Trans. Audio, Speech and Lang. Process.*, vol. 35, no. 1, pp. 118–120, January 1987.

[8] J. S. Abel and D. P. Berners, "Discrete-time shelf filter design for analog modeling," in *Proc. 115th AES Convention*, New York, USA, October 2003, paper no. 5939.

[9] F. Fontana and M. Karjalainen, "A digital bandpass/bandstop complementary equalization filter with independent tuning characteristics," *IEEE Signal Process. Letters*, vol. 10, no. 4, pp. 119–122, April 2003.

[10] T. van Waterschoot and M. Moonen, "A pole-zero placement technique for designing second-order IIR parametric equalizer filters," *IEEE Trans. Audio, Speech and Lang. Process.*, vol. 15, no. 8, pp. 2561–2565, November 2007.

[11] J. D. Reiss, "Design of audio parametric equalizer filters directly in the digital domain," *IEEE Trans. Audio, Speech and Lang. Process.*, vol. 19, no. 6, pp. 1843–1848, August 2011.

[12] S. Särkkä and A. Huovilainen, "Accurate discretization of analog audio filters with application to parametric equalizer design," *IEEE Trans. Audio, Speech and Lang. Process.*, vol. 19, no. 8, pp. 2486–2493, November 2011.

[13] J. Parker and S. D'Angelo, "A digital model of the Buchla lowpass-gate," in *Proc. 16th Intl. Conf. Digital Audio Effects (DAFx-13)*, Maynooth, Ireland, September 2013, pp. 278–285.

[14] W. Pirkle, "Modeling the Korg35 lowpass and highpass filters," in *Proc. 135th AES Convention*, New York, USA, October 2013.

[15] D. T. Yeh and J. O. Smith, "Discretization of the '59 Fender Bassman tone stack," in *Proc. 9th Intl. Conf. Digital Audio Effects (DAFx-06)*, Montreal, Canada, September 2006, pp. 189–196.

[16] K. Dempwolf, M. Holters, and U. Zölzer, "Discretization of parametric analog circuits for real-time simulations," in *Proc. 13th Intl. Conf. Digital Audio Effects (DAFx-10)*, Graz, Austria, September 2010.

[17] L. Gabrielli, V. Välimäki, H. Penttinen, S. Squartini, and S. Bilbao, "A digital waveguide-based approach for Clavinet modeling and synthesis," *EURASIP J. Advances Signal Process.*, 2013.

[18] A. Huovilainen, "Non-linear digital implementation of the Moog ladder filter," in *Proc. 7th Intl. Conf. Digital Audio Effects (DAFx-04)*, Naples, Italy, October 2004, pp. 61–64.

[19] T. E. Stinchcombe, "Derivation of the transfer function of the Moog ladder filter," 2005, available online at http://www.sdiy.org/destrukto/notes/moog_ladder_tf.pdf, accessed 08 April 2014.

[20] ——, "Analysis of the Moog transistor ladder and derivative filters," 2008, available online at http://www.timstinchcombe.co.uk/synth/Moog_ladder_tf.pdf, accessed 08 April 2014.

[21] S. D'Angelo and V. Välimäki, "An improved virtual analog model of the Moog ladder filter," in *Proc. Intl. Conf. on Acoustics, Speech, and Signal Process. (ICASSP 2013)*, Vancouver, Canada, May 2013.

[22] T. Stilson and J. O. Smith, "Analyzing the Moog VCF with considerations for digital implementation," in *Proc. Intl. Computer Music Conf. (ICMC 1996)*, Hong Kong, August 1996, pp. 398–401.

[23] F. Fontana, "Preserving the structure of the Moog VCF in the digital do-

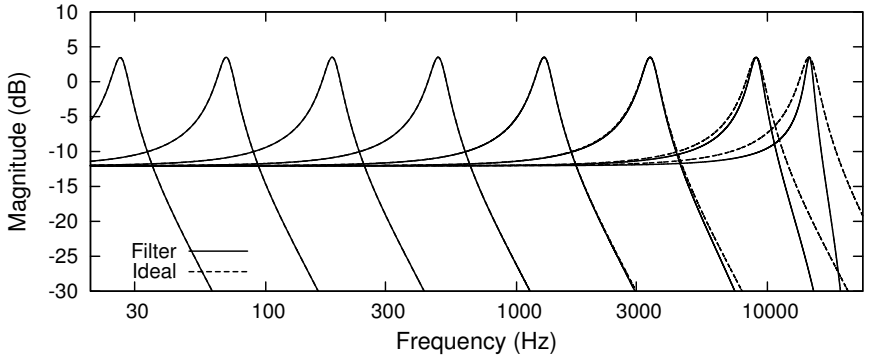


Fig. 8. Magnitude responses obtained from the fourth-order ($N = 4$) variant of the proposed filter design with $f_\mathrm{s} = 48\,\mathrm{kHz}$, $f_\mathrm{c} = 26.5\,\mathrm{Hz}$, $70.0\,\mathrm{Hz}$, $185.2\,\mathrm{Hz}$, $489.9\,\mathrm{Hz}$, $1296.1\,\mathrm{Hz}$, $3428.9\,\mathrm{Hz}$, $9071.6\,\mathrm{Hz}$, $14755.3\,\mathrm{Hz}$, and $k = 3$.

main," in *Proc. Intl. Computer Music Conf. (ICMC 2007)*, Copenhagen, Denmark, August 2007, pp. 291–294.

[24] J. O. Smith, "Signal processing library for Faust," in *Proc. Linux Audio Conf.*, Stanford, CA, USA, April 2012, pp. 153–161.

[25] D. Rossum, "Making digital filters sound analog," in *Proc. Intl. Computer Music Conf. (ICMC 1992)*, San Jose, CA, USA, October 1992, pp. 30–34.

[26] V. Välimäki and A. Huovilainen, "Oscillator and filter algorithms for virtual analog synthesis," *Comput. Music J.*, vol. 30, no. 2, pp. 19–31, June 2006.

[27] T. Hélie, "On the use of Volterra series for real-time simulations of weakly nonlinear analog audio devices: Application to the Moog ladder filter," in *Proc. 9th Intl. Conf. Digital Audio Effects (DAFx-06)*, Montreal, Canada, September 2006, pp. 7–12.

[28] ——, "Volterra series and state transformation for real-time simulations of audio circuits including saturations: Application to the Moog ladder filter," *IEEE Trans. Audio, Speech and Lang. Process.*, vol. 18, no. 4, pp. 747–759, May 2010.

[29] R. Trausmuth and A. Huovilainen, "POWERWAVE - a high performance single chip interpolating wavetable synthesizer," in *Proc. 8th Intl. Conf. Digital Audio Effects (DAFx-05)*, Madrid, Spain, September 2005, pp. 293–296.

[30] P. Daly, "A comparison of virtual analogue Moog VCF models," Master's thesis, University of Edinburgh, Edinburgh, UK, August 2012, available online at http://www.acoustics.ed.ac.uk/wp-content/uploads/AMT_MSc_FinalProjects/2012__Daly__AMT_MSc_FinalProject_MoogVCF.pdf.

[31] M. Civolani and F. Fontana, "A nonlinear digital model of the EMS VCS3 voltage-controlled filter," in *Proc. 11th Intl. Conf. Digital Audio Effects (DAFx-08)*, Espoo, Finland, September 2008, pp. 35–42.

[32] F. Fontana and M. Civolani, "Modeling of the EMS VCS3 voltage-controlled filter as a nonlinear filter network," *IEEE Trans. Audio, Speech and Lang. Process.*, vol. 18, no. 4, pp. 760–772, May 2010.

[33] S. Zambon and F. Fontana, "Efficient polynomial implementation of the EMS VCS3 filter model," in *Proc. 14th Intl. Conf. Digital Audio Effects (DAFx-11)*, Paris, France, September 2011, pp. 287–290.

[34] J. Pakarinen, V. Välimäki, F. Fontana, V. Lazzarini, and J. S. Abel, "Recent advances in real-time musical effects, synthesis, and virtual analog models," *EURASIP J. Advances Signal Process.*, pp. 1–15, 2011.

[35] P. Dutilleux, M. Holters, S. Disch, and U. Zölzer, "Filters and delays," in *DAFX: Digital Audio Effects, Second Edition*, U. Zölzer, Ed. Chichester, UK: Wiley, 2011, pp. 47–81.

[36] J. O. Smith, *Introduction to Digital Filters with Audio Applications*. http://www.w3k.org/books/: W3K Publishing, 2007, available online at http://ccrma.stanford.edu/~jos/filters/.

[37] J. Laroche, "On the stability of time-varying recursive filters," *J. Audio Eng. Soc.*, vol. 55, no. 6, pp. 460–471, June 2007.

**Stefano D'Angelo** was born in Vallo della Lucania, Italy, in 1987. He received the M.S. degree in Computer Engineering from Politecnico di Torino, Turin, Italy, in 2010. In 2009-2010, he was an Erasmus exchange student at the Helsinki University of Technology, Espoo, Finland. He is currently a doctoral student at the Department of Signal Processing and Acoustics at the Aalto University, School of Electrical Engineering, Espoo, Finland. His main research interests are audio programming languages and digital emulation of electric audio circuits.

**Vesa Välimäki** (S90–M92–SM99) received the M.S. (Tech.), the Licentiate of Science in Technology, and the Doctor of Science in Technology degrees, all in electrical engineering, from the Helsinki University of Technology (TKK), Espoo, Finland, in 1992, 1994, and 1995, respectively.

He was a Postdoctoral Research Fellow at the University of Westminster, London, UK, in 1996. In 1997-2001, he was a Senior Assistant (cf. Assistant Professor) at the TKK Laboratory of Acoustics and Audio Signal Processing, Espoo, Finland. From 1998 to 2001, he was on leave as a Postdoctoral Researcher under a grant from the Academy of Finland. In 2001-2002, he was Professor of signal processing at the Pori unit of the Tampere University of Technology, Pori, Finland. He was appointed Docent in signal processing at the Pori unit of the Tampere University of Technology in 2003. In 2006-2007, he was the Head of the TKK Laboratory of Acoustics and Audio Signal Processing. He is currently Professor in the Department of Signal Processing and Acoustics, Aalto University, Espoo, Finland. In 2008-2009, he was on sabbatical as a Visiting Scholar at the Center for Computer Research in Music and Acoustics (CCRMA), Stanford University, Stanford, CA. His research interests include audio effects processing, digital filtering, sound synthesis, and acoustics of musical instruments.

Prof. Välimäki is a senior member of the IEEE, a fellow of the Audio Engineering Society, a member of the Finnish Musicological Society, and a life member of the Acoustical Society of Finland. In 2000-2001, he was Secretary of the IEEE Finland Section. He was President of the Finnish Musicological Society in 2003-2005. In 2008, he was the Chairman of DAFx-08, the 11th International Conference on Digital Audio Effects (Espoo, Finland). He has served as an Associate Editor of the IEEE TRANSACTIONS ON AUDIO, SPEECH AND LANGUAGE PROCESSING and of the IEEE SIGNAL PROCESSING LETTERS. He was the Lead Guest Editor of a special issue of the IEEE SIGNAL PROCESSING MAGAZINE in 2007 and of a special issue of the IEEE TRANSACTIONS ON AUDIO, SPEECH AND LANGUAGE PROCESSING in 2010. He is a member of the Audio and Acoustic Signal Processing Technical Committee of the IEEE Signal Processing Society.